



ELSEVIER

Nuclear Instruments and Methods in Physics Research A 404 (1998) 315–326

**NUCLEAR  
INSTRUMENTS  
& METHODS  
IN PHYSICS  
RESEARCH**  
Section A

## Performance of fine-mesh photomultiplier tubes designed for an undoped-CsI endcap photon detector

T.K. Komatsubara<sup>a,\*</sup>, T. Morimoto<sup>a</sup>, K. Omata<sup>a</sup>, S. Sugimoto<sup>a</sup>, K. Tauchi<sup>a</sup>, T. Inagaki<sup>b</sup>, S. Kabe<sup>b</sup>, M. Kobayashi<sup>b</sup>, Y. Kuno<sup>b</sup>, T. Sato<sup>b</sup>, T. Shinkawa<sup>b</sup>, Y. Yoshimura<sup>b</sup>, I.-H. Chiang<sup>c</sup>, S. Kettell<sup>c</sup>, K.K. Li<sup>c</sup>, L.S. Littenberg<sup>c</sup>, A. Yamashita<sup>c,1</sup>, H. Suzuki<sup>d</sup>, S. Suzuki<sup>d</sup>

<sup>a</sup> High Energy Accelerator Research Organization (KEK), Tanashi-branch, 3-2-1 Midori-cho, Tanashi-shi, Tokyo 188, Japan

<sup>b</sup> High Energy Accelerator Research Organization (KEK), 1-1 Oho, Tsukuba-shi, Ibaraki 305, Japan

<sup>c</sup> Brookhaven National Laboratory, Upton, NY 11973, USA

<sup>d</sup> Electron Tube Center, Hamamatsu Photonics K.K., 314-5 Shimokanzo, Toyooka-mura, Iwata-gun, Shizuoka 438-01, Japan

Received 11 September 1997

### Abstract

We have developed two types of fine-mesh photomultiplier tubes for an undoped-CsI endcap photon detector installed in a strong axial magnetic field. These photomultiplier tubes have ultraviolet-transmitting glass windows, backed by large-area bialkali photocathodes, in order to efficiently detect scintillation light from undoped-CsI crystals. A gain of more than  $2 \times 10^5$ , in a magnetic field of 1.0 T, was obtained from these tubes with 19-stage fine-mesh dynodes. Gain drops caused by the magnetic field and by high anode currents were investigated. Several performance criteria of the tubes were studied: gain, quantum efficiency, linearity, noise, and transit time spread. © 1998 Elsevier Science B.V. All rights reserved.

PACS: 13.20.Eb; 29.40.Mc; 29.40.Vj; 85.60.Ha

Keywords: Fine-mesh photomultiplier tube; Magnetic field; Gain; Undoped-CsI; Endcap; E787

### 1. Introduction

Fine-mesh photomultiplier tubes (PMTs) which can be used in high magnetic fields ( $\geq 1$  T) have recently been developed by Hamamatsu [1], and

tested by several groups [2–7] aiming to apply them to time-of-flight, Cherenkov, and calorimetric counters in various magnetic spectrometers. The unique performance of these PMTs was obtained from a fine-mesh dynode structure, where each fine-mesh layer is separated by a narrow gap, and the first layer is placed very close to the photocathode so as to efficiently trap and multiply photoelectrons traversing along spiral trajectories in a high magnetic field. The unique dynode structure

\* Corresponding author. Tel.: +81 424 69 9549; fax: +81 424 62 0775; e-mail: takeshi.komatsubara@kek.jp.

<sup>1</sup> Present address: SPring-8, Kamigori, Ako-gun, Hyogo 678-12, Japan.

offers additional benefits such as a short transit time and small time jitter. Although several feasibility studies concerning the fine-mesh PMT have been made, quantitative studies based on the testing of a large number of PMTs have not been reported.

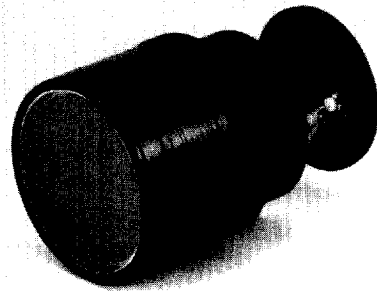
We have developed new-type fine-mesh PMTs for a rare kaon decay experiment at Brookhaven National Laboratory (BNL) (E787 – A search for the  $K^+ \rightarrow \pi^+ \nu \bar{\nu}$  decay [8–18]) and investigated the performance. Our test of  $\sim 200$  PMTs included measurements of: (1) the quantum efficiency, (2) the gain, (3) the linearity, (4) the gain drop in high-rate background environments, and (5) the gain drop and noise in high magnetic fields. In this paper we report on the quantitative results of these measurements.

## 2. Design of the PMTs

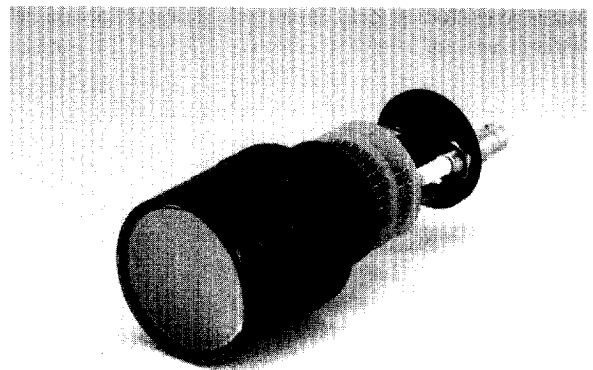
Two types of PMTs (3 in type: R5543 [19], 2 in type: R5545 [20]) were specially designed so as to meet the requirement of upgrading the endcap photon detector of the rare kaon decay experiment E787 at BNL [21]. The main role of the endcap detector is to efficiently veto low-energy photons (a few – 230 MeV) in the 1.0 T axial field of the E787 solenoid magnet. The endcap detector operates in the high-rate environment of secondary particles produced by the high-intensity stopping  $K^+$  beam ( $\sim 10^7 K^+ / 1.6$  s) [22]. The endcap detector is required to have good timing resolution to reduce losses from accidental vetoes, and high sensitivity for photon detection in the field of 1.0 T. Any blindness of the endcap system due to accidentals must be small. The signal output should be greater than several tens of photo-electrons per MeV to give a time resolution better than 1 ns. To fulfill these requirements, E787 has chosen undoped cesium iodide (undoped-CsI) as the scintillation material. This crystal is known to have fast response and high light output [23]. The PMT of fine-mesh dynodes was chosen as the photo-sensor for this scintillator due to its good timing response, efficient light collection, and large gain in the magnetic field.

The 3 in and 2 in PMTs have ultraviolet-transmitting glass (UV-glass) windows and bialkali

photocathodes to detect the undoped-CsI scintillation light at wavelengths ( $\lambda$ ) of around 300 nm. The light output from each crystal is measured by a PMT through a 3 mm thick UV-transparent silicone cookie [24] and a UV band-pass filter [25]. The filter is used to select the fast component from the scintillation of the undoped-CsI (fast component:  $\lambda \sim 300$  nm, slow component:  $\lambda \sim 450$  nm). The photocathode of the 3 in (2 in) PMT is 64 mm (43 mm) in diameter; the area-ratio of the photocathode to the window is 67% (68%). To achieve high enough gain to detect low-energy photons, 19-stage fine-mesh (1500 wires/in) dynodes were



(a)



(b)

Fig. 1. (a) R5543 (3 in) and (b) R5545 (2 in) fine-mesh PMTs. Ultraviolet transmitting glass window and bialkali photocathode are used. The PMT is wrapped first with white Teflon tape and then with black electrical tape. A high-voltage dividing circuit board is mounted on the rear end of the PMT. The black plastic ring is a part of the PMT mounting structure.

Table 1  
Characteristic parameters of R5543 and R5545

Type of PMT	R5543 (3 in.) (R5545 (2 in.))
Dynode type	Fine mesh 1500 wires/in
Number of dynode stages	19
PMT diameter	78 (52) mm
Photocathode diameter	> 64 (> 43) mm
PMT length	51 (46) mm
PMT length with high-voltage divider	123.7 (124.1) mm
Window	UV-glass
Photocathode	Bialkali
Active region of wavelength	200–600 nm
Quantum efficiency at $\lambda = 280$ nm	> 11%
Quantum efficiency at $\lambda = 300$ nm	> 13%
Quantum efficiency at $\lambda = 320$ nm	> 16%
High voltage required for the gain of $2 \times 10^7$ at 0 field	< 2500 V

used. A high-voltage dividing circuit, designed for high anode currents (a few tens  $\mu\text{A}$ ) caused by the high flux of incident particles, was mounted directly on the rear end of the PMT by the manufacturer (see Fig. 1). The characteristic parameters of the PMTs are summarized in Table 1.

There are 143 crystals in the endcap detector [26]: 75 blocks in the upstream and 68 blocks in the downstream. The coverage of the 3 in (2 in) PMTs is about 63% (56%) of the crystal face. The 2 in PMTs (13 in the upstream and 11 in the downstream) are mounted on the crystals of the innermost cylindrical layer of the endcap detector; the 3 in PMTs (62 in the upstream and 57 in the downstream) are mounted on the outer 3 layers.

### 3. Performance

All of the PMTs fabricated for the E787 endcap detector were tested with and without magnetic fields prior to the assembly. The quantum efficiency of each PMT was determined by measuring the average number of photo-electrons emitted from the cathode, divided by the number of incident photons in a monochromatic pulsed beam with a diameter of 25 mm. The spectral response of

the photocathode was measured at three different wavelengths:  $\lambda = 280, 300,$  and  $320$  nm. Fig. 2 shows the measured quantum efficiencies: all are greater than 13% at  $\lambda = 300$  nm.

The current amplification, i.e. gain ( $G$ ), of a PMT can be expressed as a function of the applied voltage ( $V$ ):

$$G = K \times V^{\alpha n},$$

where  $K$  is a constant,  $n$  is the number of dynode stages ( $n = 19$ ), and  $\alpha$  is a coefficient determined by the dynode material and geometrical structure [1]. The measured values of  $\alpha n$  are shown in Fig. 3, where  $\alpha n$  of each PMT was determined by fitting the above formula to the output induced by a standard light-pulse at five different applied voltages. The mean value of  $\alpha n$  for the 3 in PMTs,  $\approx 8.2$ , is consistent with that for the 2 in PMTs.

The high voltage applied to a PMT to yield a gain of  $2 \times 10^7$  at zero magnetic field is defined as the equivalence voltage (EqV), which is required to be below the maximum voltage of the PMT (2500 V). The measured EqV's are shown in Fig. 4. The PMTs are all expected to have gains of  $> 2 \times 10^5$  at EqV in a magnetic field of 1.0 T, since the gain drops are expected to be less than a factor 100 (see Section 5). The absolute gain is derived from the ratio of the anode output current to the photo-electric current from the cathode irradiated by a white light beam of W-2856 K with a diameter of 60 mm (40 mm) for the 3 in (2 in) PMTs.

The output linearity at (EqV – 300) V was measured by changing the intensity of the input light-pulse. The deviation from linearity was found to be less than 0.5% up to an anode charge of 2000 pC, which corresponds to about 1.3 GeV energy deposit in an endcap crystal.

### 4. Gain drift caused by DC light background

Since the endcap detector is located close to the high-flux beam line, and consequently the anode current while the beam is on is expected to be a few  $\mu\text{A}$ , the short- and long-term gain drifts of the PMTs caused by high anode currents were carefully investigated.

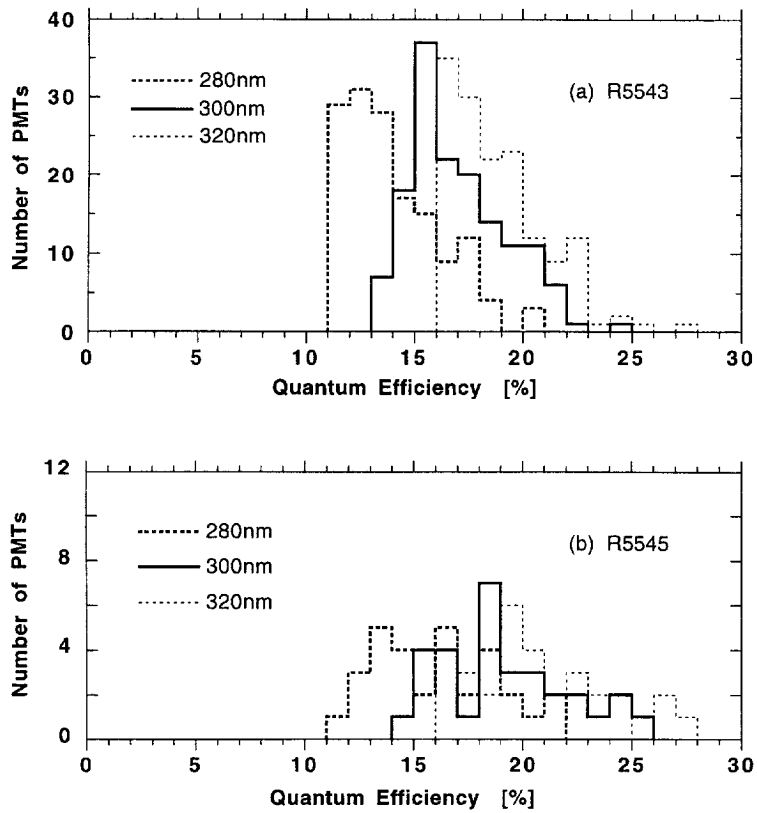


Fig. 2. Distribution of quantum efficiency at three wavelengths: (a) the measured quantum efficiency for the 3 in PMTs and (b) for the 2 in PMTs.

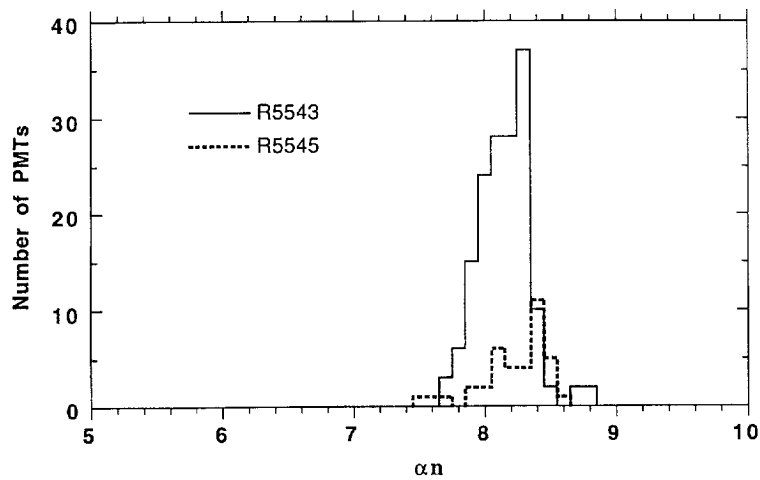


Fig. 3. Distribution of  $\alpha n$ . The solid (dotted) histogram shows the measured values of  $\alpha n$  for the 3 in (2 in) PMTs.

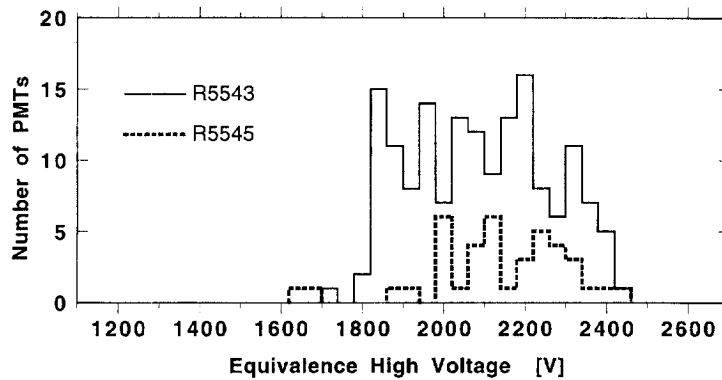


Fig. 4. Distribution of the equivalence voltage EqV. The solid (dotted) histogram shows the applied high voltage on the PMTs necessary to obtain a gain of  $2 \times 10^7$  without magnetic fields for the 3 in (2 in) PMTs.

#### 4.1. Short-term gain drift

All of the PMTs were examined using an automatic test system at INS<sup>2</sup> [27,28]. The system has two kinds of light sources: a xenon flash lamp, which produces light-pulses to simulate scintillation light at a rate of 10 Hz, and a tungsten lamp, which produces DC light to vary the anode current. The pulsed light and the background DC light are mixed and distributed to the front face of the PMTs through glass fibers. The light intensity of the xenon lamp is monitored by 8 reference PMTs (Hamamatsu R580-12). The signals from these PMTs are sent to CAMAC analog-to-digital converters (Hohshin ADC C009: 1000 pC/4096 ch). A 500 ns ADC gate is triggered by a PIN photodiode monitoring the xenon lamp. The intensity of the background light is varied by changing the voltage applied to the tungsten lamp. The entire system is controlled by a personal computer (NEC-PC9800). The details of the system are described elsewhere [27,28].

Fig. 5 shows a typical short-term gain-drift caused by the DC light background, which was applied during the time interval 18–66 h. The relative gain shown in the figure was derived by

measuring the PMT output induced by the standard xenon light-pulse. To understand the gain drift in detail we measured the pulse-height of the output at the PMT voltage of 1800 and 2000 V over a wide range of DC light intensities by using four steps of optical filters. Fig. 6 demonstrates that the relative gains fall on a smooth curve as a function of the anode current: monotonically decreasing as the anode current increases.

The test procedure consists of several steps. Each PMT at the EqV is left for 24 h without any input light for primary aging. Then a PMT-stability test is initiated (at 0 h in Fig. 5): the PMT voltage is set

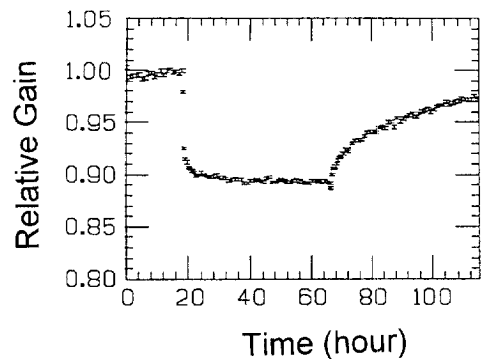


Fig. 5. Typical gain drop in DC background light. The DC background light was applied on the PMT during the time interval 18–66 h.

<sup>2</sup> The former Institute for Nuclear Study of the University of Tokyo. INS was re-organized to be the Tanashi-branch of High Energy Accelerator Research Organization in April of 1997.

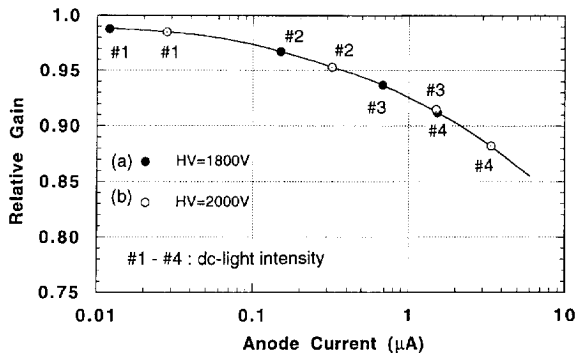


Fig. 6. Relative gain versus the anode current at an applied voltage of (a) 1800 V and (b) 2000 V. The PMT gain was measured using a standard light pulser, while applying a DC light background whose intensity was changed with four different optical filters (#1–#4). All of the data points are on a single curve expressed as a function of the anode current.

to be  $(EqV - 300)V$ , with a gain of  $(5-7) \times 10^6$ , so as to induce an anode current of a few  $\mu A$  with the tungsten lamp. The gain drift is monitored by measuring the pulse height of the output signal induced by the standard light pulse for 18 h without any DC light background, and then for 48 h with a DC light background. The mean value of the pulse height is obtained every 30 min by measuring 2000 pulses with the ADC. The relative gain is corrected for the drift of the xenon-lamp output, which is monitored by the reference PMTs. After taking data on the DC background, the tungsten lamp is turned off and measurements are continued for the next 72 h. Subsequently, the light intensity of the tungsten lamp is reduced to 60% of the previous value and the measurement repeated. This procedure is repeated until the gain becomes stable ( $\pm 0.5\%/10h$ ) in both cases, with and without background light.

Fig. 7 shows the relative gain of the PMTs for an anode current of  $1 \mu A$  normalized by the gain with negligibly low anode current. More than 80% of the 3 in (2 in) PMTs exhibit a gain drop of less than 10% (15%). The gain drop of the 2 in PMTs is larger than that of the 3 in PMTs. This is considered to be due to the difference in their current density on the last dynode, i.e. the current density of the 2 in PMT is higher by a factor of 2.2 than that of the 3 in PMT.

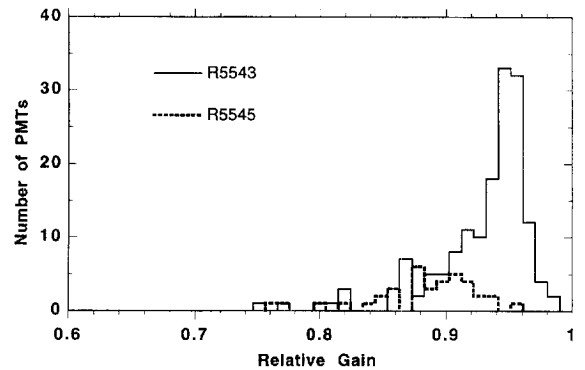


Fig. 7. Distribution of relative gains with an anode current of  $1 \mu A$ , normalized by the gain without significant anode current. The solid (dotted) histogram shows the gain of the 3 in (2 in) PMT.

The time constant of the gain drop or that of the gain recovery for each PMT was derived by fitting an exponential curve to the data. Fig. 8 shows the distributions of the measured time constant of the gain drops. There are 91 PMTs (3 in) with time constants in a range between 18 and 42 min, and 8 in a range between 1 and 5 min. One PMT has an extremely short time constant of 0.6 min. The shortest time constant of the gain drop for the 2 in PMTs is 14 min. Regarding the gain recovery, there exist two components: a short time constant ( $\tau_1$ ) and a long time constant ( $\tau_2$ ). The distributions of those measured time constants are shown in Fig. 9(a) and Fig. 9(b). Among the 197 PMTs, one 3 in PMT has a very short time constant of 2.2 min. Special care should be taken in using these PMTs with such short time constants. All correlations between the time constants and the PMT gain (or gain drift) were examined in order to analyze the factors leading to such short time constants, but none of significance was found.

In the E787 experiment, accelerated protons are extracted from the Alternating Gradient Synchrotron (AGS) for about 1.6 s in every 3.6 s. To simulate the gain drop with conditions similar to the AGS spill structure, we tested the gain by measuring a standard xenon light-pulse while illuminating the PMT with an LED for 1 s in every 3 s. The result of the measurement showed that the gain

drop caused by the LED (duty factor = 1/3) was equivalent to that caused by continuous LED light with one-third of the intensity. The gain drift therefore depends only on the average anode current for time constant significantly greater than the repetition period.

4.2. Long-term gain drift in a high-rate beam environment

To investigate long-term gain drift, we tested a sample of 13 PMTs (3 in) with a high anode current. The test was carried out at Hamamatsu

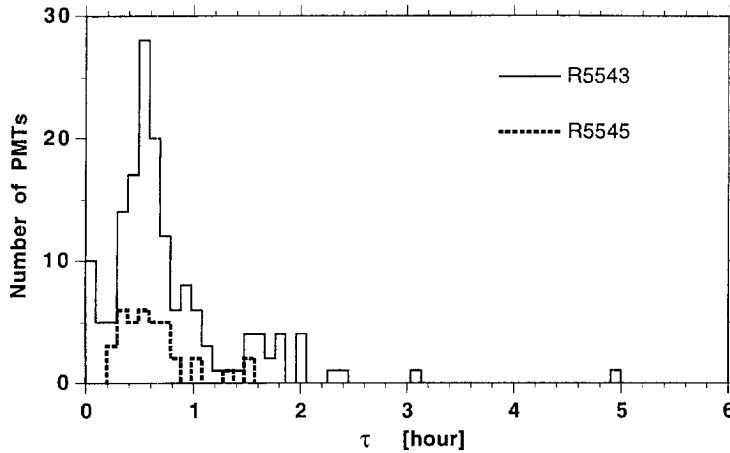


Fig. 8. Distribution of the time constant of the gain drop caused by an anode current of 1  $\mu$ A. The time constant ( $\tau$ ) was derived from an equation ( $\text{gain} = (b - a)\exp(-t/\tau) + a$ ) fitted to the data of gain drop. The solid (dotted) histogram shows the time constant for the 3 in (2 in) PMTs.

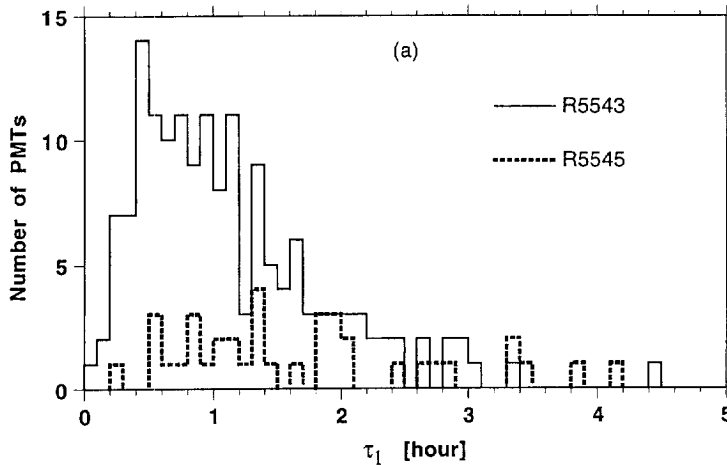


Fig. 9. Distribution of the two components of the time constant of the gain recovery. The short component ( $\tau_1$ ) and the long component ( $\tau_2$ ) are shown in (a) and (b), respectively. These time constants were derived from an equation ( $\text{gain} = a_0 - a_1 \exp(-t/\tau_1) - a_2 \exp(-t/\tau_2)$ ) fitted to the data of gain recovery. The solid (dotted) histogram shows the time constant for the 3 in (2 in) PMTs. In (b),  $\tau_2 = 100$  h is assigned as an overflow bin ( $\tau_2 \geq 100$  h).

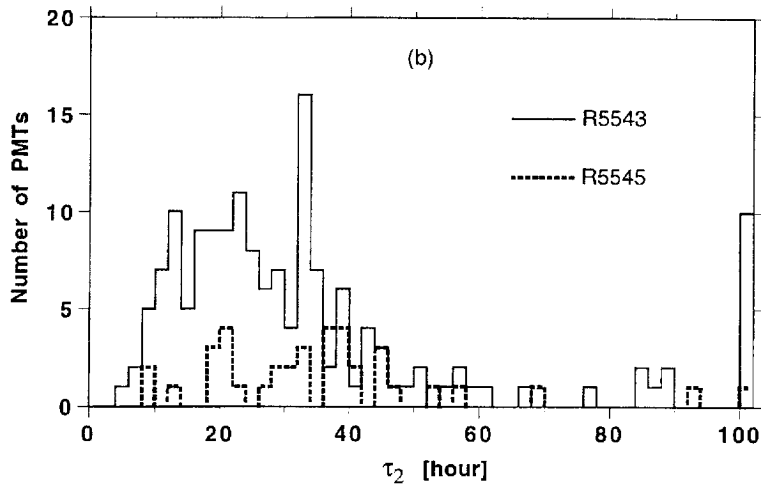


Fig. 9. (Continued).

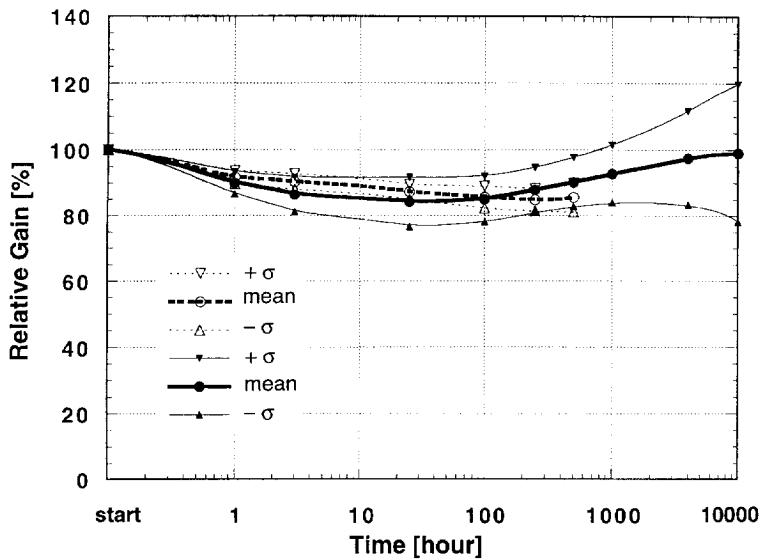


Fig. 10. Long-term gain drift in a high-background anode current. The solid (dotted) curve shows the gain at an anode current of  $100\ \mu\text{A}$  ( $10\ \mu\text{A}$ ). The lines of  $\pm 1\sigma$  show the deviation from the mean of the relative gains of the 5(8) PMTs.

with a DC tungsten lamp to induce high anode currents. A sample of 5 PMTs were tested with an anode current of  $10\ \mu\text{A}$  for 5000 h, and a sample of 8 PMTs were tested in  $100\ \mu\text{A}$  for 10000 h. In the early stages (the first 500 h for  $10\ \mu\text{A}$  and the first 50 h for  $100\ \mu\text{A}$ ), the gain dropped smoothly to an average of 85%, and then increased. After 500 h at

$100\ \mu\text{A}$ , the 8 PMTs varied widely in gain without any particular tendency. At 10000 h the gain scattered between 78.2 and 119.8% with an average of 99.0% and a root-mean-squared (rms) of 20.8%. The data shown in Fig. 10 indicate that the PMTs with an anode current of  $100\ \mu\text{A}$  are usable for a period of 10000 h, if a slow gain variation of

$\sim \pm 30\%$  is acceptable. On the assumption that this long-term aging effect is proportional to its integrated anode current, an anode current of  $100\ \mu\text{A}$  for 10 000 h is equivalent to the maximum expected level for 4 full years of operation for the E787 endcap detector. The durability of the PMTs against a high flux of incident particles therefore meets the requirement of the E787 experiment. To cope with the gain variation, E787 has installed a gain-monitoring system incorporating a xenon flash lamp with an accuracy of 2% [29].

**5. Gain in magnetic fields**

All of the PMTs fabricated for the E787 experiment were also tested at KEK in high magnetic fields. Their gains were measured using a standard light pulser,  $\text{YAlO}_3(\text{Ce})$  scintillator with  $^{241}\text{Am}(5.49\ \text{MeV}\ \alpha)$ , whose light intensity does not change in a magnetic field of 1 T [30,31]. The light pulser has a diameter of 3.0 mm and was mounted at a distance of 12 mm from the PMT window. The PMT under test was set in a wide-gap dipole magnet parallel to the magnetic field at a high-voltage of  $(E_{\text{qV}} - 300)\text{V}$ . The relative gains in magnetic fields of 0.0, 0.25, 0.5, 0.75, 0.95, 1.00 and 1.05 T were measured using a LeCroy 2249W CAMAC ADC module with a gate width of 200 ns. In Fig. 11 the gain drop of a sample of ten PMTs is shown as a function of the magnetic field. The gain of a wire-

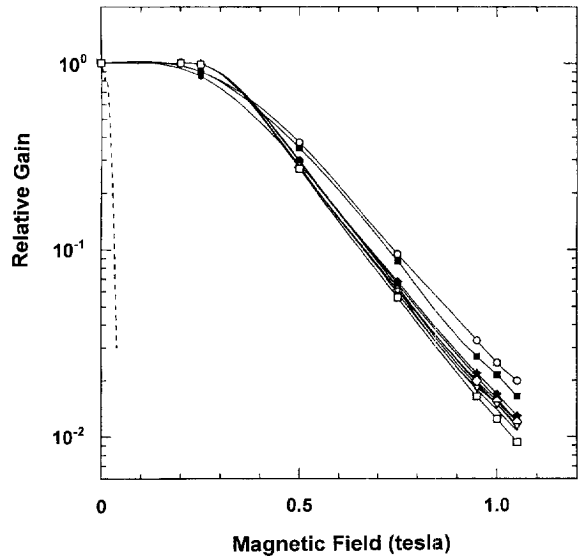


Fig. 11. Gain drop in magnetic fields. The gain as a function of magnetic field (parallel to the PMT axis) is shown for a sample of 10 PMTs (R5543). The broken line indicates the gain of a wire-mesh PMT [32].

mesh PMT [32], which can be operated upto order of 100 G, is shown as a reference. Fig. 12 shows the measured relative gains at 1.00 T for all of the PMTs. The average of relative gains for the 3 in (2 in) PMTs is 0.016 (0.014). There are a few PMTs that are extremely resistant to the magnetic field, whose relative gains are higher than 0.05. The

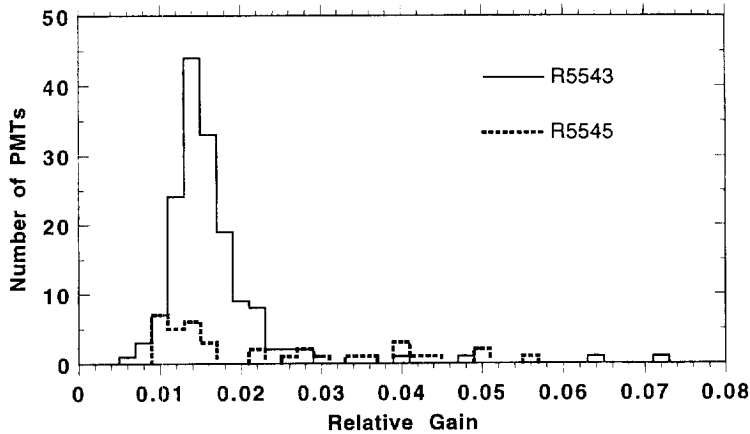


Fig. 12. Gain in a 1.00 T axial field (relative to  $B = 0$ ).

relative gain in a 1.00 T field is greater than 0.01 for 95% of the 3 in PMTs and 90% of the 2 in PMTs.

## 6. Noise and transit time spread in magnetic fields

The fine-mesh PMT is known to have a peculiarity: single photo-electron signals make double or triple peaks in a pulse-height distribution [7,33,34], because only 40% of single photo-electrons emitted from the photocathode hit the first layer of fine-mesh dynode and the remaining 60% of them pass through the mesh-holes of the first dynode without hitting it. Thus the PMT has an intrinsic noise that is worse than the noise of an ordinary PMT (e.g. Hamamatsu R329 with a box-and-grid anode structure).

In order to compare the intrinsic noise of this type of PMT with that of an ordinary one at zero magnetic field, we measured the energy resolution of the  $\text{YAlO}_3(\text{Ce})$  that was directly mounted on the PMT with transparent optical grease (OKEN 6262). The number of photo-electrons produced by the  $\text{YAlO}_3(\text{Ce})$  light pulser was estimated to be about 2000. A typical resolution measured with the 3 in (2 in) PMT was 3.1%(3.5%). On the other hand the resolution measured with the R329 was 2.5%. This data shows an excess of the noise component in the electron multiplication process of the

fine-mesh PMT : the effective number of photo-electrons is about half that observed with an ordinary PMT.

The additional noise due to magnetic field was also investigated by comparing the fluctuation of the pulse-height at 1.00 T of axial field ( $\sigma_{1T}$ ) with that at 0 T ( $\sigma_{0T}$ ). A  $\text{YAlO}_3(\text{Ce})$  was mounted at a distance of 12 mm from the PMT window, as mentioned in Section 5. The number of photo-electrons was 300–400 and the 3 in (2 in) PMT had a resolution of  $\sigma_{0T} = 6.7\%(7.7\%)$ . The degradation due to the magnetic field was small : as shown in Fig. 13(a) and Fig. 13(b), the ratio  $\sigma_{1T}/\sigma_{0T}$  for the 3 in (2 in) PMTs scattered between 0.750 (0.875) and 1.250 (1.175), with an average of 1.027 (1.024) and a rms of 0.069 (0.055). This small effect is consistent with the results reported by a recent article [7]. The pulse shape of output signals from the PMT in a 1 T field was compared with that in a 0 T field, and no clear deterioration was observed.

The transit time spread (TTS) for a single photo-electron was measured in high magnetic fields by using laser pulses through a few layers of diffusers in order to control their intensity. Fig. 14 shows the TTS for a sample of 3 PMTs (3 in) in various magnetic fields. The measured TTS in an axial field ( $\theta = 0^\circ$ ) of about 1 T indicates a rather large, but acceptably short, time spread in a range between 260 and 300 ps, while the TTS at 0 T is in a range between 130 and 160 ps.

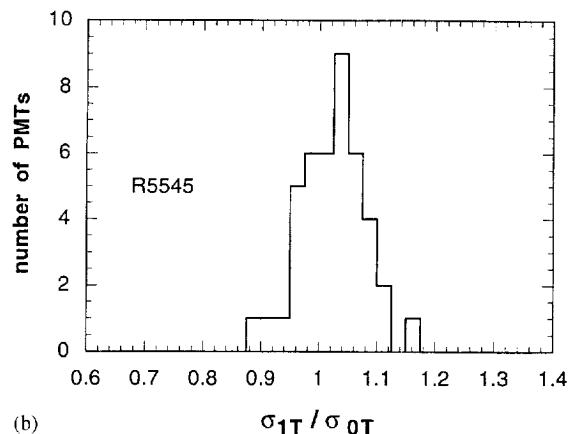
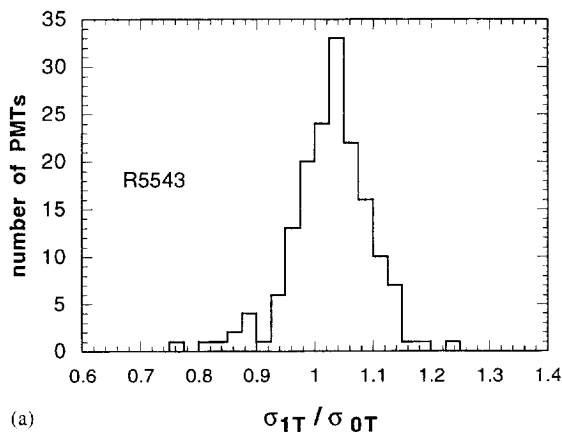


Fig. 13. Ratio of the peak width of the pulse-height distribution at 1.00 T of axial field to the width at 0 T for (a) 3 in PMTs and (b) 2 in PMTs.

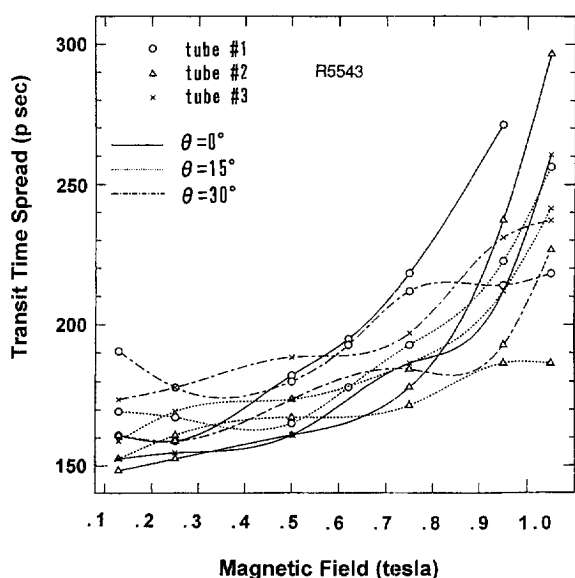


Fig. 14. Transit time spread for a single photo-electron in high magnetic fields.  $\theta$  indicates the angle of the PMT to the magnetic field. The curves through the data points are drawn to guide the eye. The error of each data point is estimated to be smaller than 10 ps.

## 7. Conclusions

We have developed two types of fine-mesh PMTs for the undoped-CsI endcap detector in the experiment E787 and measured the performance of  $\sim 200$  PMTs. Each of these PMTs showed a gain of  $2 \times 10^7$  for a high voltage below 2500 V at zero magnetic field. The effect of the anode current on the gain was carefully investigated. The gain drop, which depends on the average current of the anode output, was less than 10% (15%) for 80% of the 3 in (2 in) PMTs at an anode current of  $1 \mu\text{A}$ . A few PMTs showed larger gain drops (20–25%). This result suggests that gain-monitoring is essential in precise measurements with this type of PMT in a high-rate beam environment. To cope with unstable beam conditions and large gain drops, we have developed a gain-monitoring system using a xenon flash lamp [29]. During the experiment, the gain was monitored between every beam bunch extracted from the AGS, with a precision of 2%. We also confirmed that this type of PMT is usable at an anode current of  $100 \mu\text{A}$  for a period of 10 000 h.

The gain of most of the PMTs dropped by a factor of 50–100 in a 1.0 T field, which enabled us to obtain a gain of more than  $2 \times 10^5$  in the E787 experiment. The additional noise due to magnetic field was small. The transit time spread for a single photo-electron deteriorated to 300 ps at 1 T, but it is still within the tolerance level for the E787 experiment.

These new types of PMTs have been working very well in the endcap detector since 1994 [21]. Details concerning the endcap performance will be presented elsewhere [29].

## Acknowledgements

We would like to express our thanks to the collaborators of E787 for useful discussions during this project. We also wish to acknowledge with gratitude the members of the ZEUS-Tokyo group, especially Prof. S. Yamada for his valuable advice on this PMT development and Dr. T. Ishii and Mr. K. Shiino for giving us useful information concerning how to operate their PMT test system. We are thankful to Mr. T. Hakamada for helpful discussions and supports on this project at Hamamatsu Photonics. We would like to acknowledge Mr. M. Taino and Mr. Y. Suzuki for giving us various useful help in operating the large aperture spectrometer magnet. This work was carried out under the US/Japan Cooperative Program in High Energy Physics, and was also partially supported by the Ministry of Education, Science, Sports and Culture, Grant-in-Aid for Scientific Research, and by the US Department of Energy under Contract No.DE-AC02-76 CH00016.

## References

- [1] Hamamatsu Photonics Catalogue.
- [2] F. Takasaki et al., Nucl. Instr. and Meth. 228 (1985) 369.
- [3] G. Finsel et al., Nucl. Instr. and Meth. A 290 (1990) 450.
- [4] H. Kichimi et al., Nucl. Instr. and Meth. A 325 (1993) 451.
- [5] R. Enomoto et al., Nucl. Instr. and Meth. A 332 (1993) 129.
- [6] J. Janoth et al., Nucl. Instr. and Meth. A 350 (1994) 221.
- [7] T. Iijima et al., Nucl. Instr. and Meth. A 387 (1997) 64.
- [8] M.S. Atiya et al., Phys. Rev. Lett. 63 (1989) 2177.
- [9] M.S. Atiya et al., Phys. Rev. Lett. 64 (1990) 21.

- [10] M.S. Atiya et al., Phys. Rev. Lett. 65 (1990) 1188.
- [11] M.S. Atiya et al., Phys. Rev. Lett. 66 (1991) 2189.
- [12] M.S. Atiya et al., Phys. Rev. Lett. 69 (1992) 733.
- [13] M.S. Atiya et al., Phys. Rev. Lett. 70 (1993) 2521.
- [14] M.S. Atiya et al., Phys. Rev. D 48 (1993) R1.
- [15] S. Adler et al., Phys. Rev. Lett. 76 (1996) 1421.
- [16] P. Kitching et al., Phys. Rev. Lett. 79 (1997) 4079.
- [17] S. Adler et al., hep-ex/9708012, Phys. Rev. Lett., submitted.
- [18] M.S. Atiya et al., Nucl. Instr. and Meth. A 321 (1992) 129.
- [19] The original name is Hamamatsu R5065Mod-Assy.
- [20] The original name is Hamamatsu R4721Mod-Assy, discontinued.
- [21] S. Adler et al., Phys. Rev. Lett. 79 (1997) 2204. This is a result obtained using the upgraded endcap system.
- [22] I.-H. Chiang et al., Nucl. Instr. and Meth. A, to be submitted.
- [23] S. Kubota et al., Nucl. Instr. and Meth. A 268 (1988) 275.
- [24] Sylgard 527 (Dow Corning Chemical), with a UV cutoff at  $\lambda \sim 240$  nm and 95% transmission above 350 nm.
- [25] 2.5 mm thick band-pass filter: Kenko U330. The transmitting band is  $\lambda = 230\text{--}395$  nm (fwhm), and the maximum transmittance is 90%.
- [26] I.-H. Chiang et al., IEEE Trans. Nucl. Sci. 42 (1995) 394.
- [27] K. Shiino et al., INS Technical Report INS-T-495 (1990) (INS, Univ. of Tokyo).
- [28] T. Ishii et al., Nucl. Instr. and Meth. A 320 (1992) 449. This system was constructed by ZEUS-Tokyo group.
- [29] E787 collaboration, to be published.
- [30] M. Kobayashi et al., Nucl. Instr. and Meth. A 337 (1994) 355.
- [31] The light output of  $\text{YAlO}_3(\text{Ce})$  in magnetic fields was measured with a fine-mesh PMT. The gain of the PMT in the magnetic field was calibrated by measuring the light intensity of a standard LED pulser, placed outside of the magnetic field, through a quartz fiber. Comparing those light outputs, the authors in [30] found no degradation of the  $\text{YAlO}_3(\text{Ce})$  in a magnetic field at least up to 1 T.
- [32] S. Orito et al., Nucl. Instr. and Meth. 216 (1983) 439.
- [33] K. Arisaka, T. Hakamada, F. Takasaki, private communication.
- [34] R. Suda et al., hep-ex/9707042, Nucl. Instr. and Meth. A, submitted.